



OPEN ACCESS

EDITED BY

Hedwig E. Deubzer,
Charité University Medicine Berlin,
Germany

REVIEWED BY

Nina Gelineau,
Princess Maxima Center for Pediatric
Oncology, Netherlands
David Meredith,
Harvard Medical School, United States

*CORRESPONDENCE

Eva María Trinidad

✉ eva_trinidad@iislafe.es

Jaime Font de Mora

✉ jaime.fontdemora@gmail.com

RECEIVED 05 September 2022

ACCEPTED 24 April 2023

PUBLISHED 12 May 2023








CITATION

Trinidad EM, Juan-Ribelles A, Pisano G,
Castel V, Cañete A, Gut M, Heath S and
Font de Mora J (2023) Evaluation of
circulating tumor DNA by
electropherogram analysis and methylome
profiling in high-risk neuroblastomas.
Front. Oncol. 13:1037342.
doi: 10.3389/fonc.2023.1037342

COPYRIGHT

© 2023 Trinidad, Juan-Ribelles, Pisano,
Castel, Cañete, Gut, Heath and Font de
Mora. This is an open-access article
distributed under the terms of the [Creative
Commons Attribution License \(CC BY\)](https://creativecommons.org/licenses/by/4.0/). The
use, distribution or reproduction in other
forums is permitted, provided the original
author(s) and the copyright owner(s) are
credited and that the original publication in
this journal is cited, in accordance with
accepted academic practice. No use,
distribution or reproduction is permitted
which does not comply with these terms.

Evaluation of circulating tumor DNA by electropherogram analysis and methylome profiling in high-risk neuroblastomas

Eva María Trinidad ^{1,2*}, Antonio Juan-Ribelles ^{2,3},
Giulia Pisano ^{2,3}, Victoria Castel ^{2,3}, Adela Cañete ^{2,3,4},
Marta Gut ⁵, Simon Heath⁵ and Jaime Font de Mora ^{1,2*}

¹Laboratory of Cellular and Molecular Biology, Health Research Institute Hospital La Fe, Valencia, Spain, ²Clinical and Translational Research in Cancer, Health Research Institute Hospital La Fe, Valencia, Spain, ³Pediatric Oncology Unit, La Fe University Hospital, Valencia, Spain, ⁴School of Medicine, University of Valencia, Valencia, Spain, ⁵National Center for Genomic Analysis – Centre for Genomic Regulation (CNAG-CRG), Centre for Genomic Regulation (CRG), Barcelona Institute of Science and Technology (BIST), Universitat Pompeu Fabra (UPF), Barcelona, Spain

Background: Liquid biopsy has emerged as a promising, non-invasive diagnostic approach in oncology because the analysis of circulating tumor DNA (ctDNA) reflects the precise status of the disease at diagnosis, progression, and response to treatment. DNA methylation profiling is also a potential solution for sensitive and specific detection of many cancers. The combination of both approaches, DNA methylation analysis from ctDNA, provides an extremely useful and minimally invasive tool with high relevance in patients with childhood cancer. Neuroblastoma is an extracranial solid tumor most common in children and responsible for up to 15% of cancer-related deaths. This high death rate has prompted the scientific community to search for new therapeutic targets. DNA methylation also offers a new source for identifying these molecules. However, the limited blood sample size which can be obtained from children with cancer and the fact that ctDNA content may occasionally be diluted by non-tumor cell-free DNA (cfDNA) complicate optimal quantities of material for high-throughput sequencing studies.

Methods: In this article, we present an improved method for ctDNA methylome studies of blood-derived plasma from high-risk neuroblastoma patients. We assessed the electropherogram profiles of ctDNA-containing samples suitable for methylome studies, using 10 ng of plasma-derived ctDNA from 126 samples of 86 high-risk neuroblastoma patients, and evaluated several bioinformatic approaches to analyze DNA methylation sequencing data.

Results: We demonstrated that enzymatic methyl-sequencing (EM-seq) outperformed bisulfite conversion-based method, based on the lower proportion of PCR duplicates and the higher percentage of unique mapping reads, mean coverage, and genome coverage. The analysis of the electropherogram profiles revealed the presence of nucleosomal multimers, and occasionally high molecular weight DNA. We established that 10% content of the mono-nucleosomal peak is sufficient ctDNA for successful detection of copy

number variations and methylation profiles. Quantification of mono-nucleosomal peak also showed that samples at diagnosis contained a higher amount of ctDNA than relapse samples.

Conclusions: Our results refine the use of electropherogram profiles to optimize sample selection for subsequent high-throughput analysis and support the use of liquid biopsy followed by enzymatic conversion of unmethylated cysteines to assess the methylomes of neuroblastoma patients.

KEYWORDS

liquid biopsy, high-risk neuroblastoma, DNA methylation, ctDNA / normal cfDNA ratio, enzymatic methyl-sequencing (EM-seq)

Introduction

Neuroblastoma is the most common extracranial solid tumor in children and responsible for up to 15% of cancer-related deaths (1). These tumors are heterogeneous with extreme clinical variability ranging from spontaneous regression to rapid progression and metastasis. Risk markers (histology, age, *MYCN* amplification, INRG stage, ploidy status, and 11q aberration) are used to divide patients into three categories: low, moderate, and high (2). Low and intermediate groups show greater than 90% five-year survival rates, whereas the survival of the high-risk group remains around 40%, which decreases to 10% upon relapse (3). Approximately half of all newly diagnosed neuroblastomas are designated high-risk for relapse. Therefore, there is an urgent need to develop novel treatment targets to improve the survival rate of high-risk neuroblastoma patients. Primary neuroblastoma tumors have been shown to contain a low number of coding mutations (4) suggesting that either they have very few potent oncogene/tumor suppressor drivers or that there are alternative mechanisms underlying tumorigenesis. Some high-risk neuroblastoma tumors display somatic amplifications/mutations in oncogene drivers, such as *MYCN*, *ALK*, *PTPN11*, *ATRX* and *NRAS* (5, 6). However, other high-risk neuroblastoma tumors do not harbor either *MYCN* amplification or mutations in other known tumor drivers, suggesting that perhaps epigenetic changes, such as DNA methylation, are involved in the tumorigenesis process. Large-scale genome sequencing projects have shown the importance of the epigenome to neuroblastoma (7). Recently, we have found a DNA methylation profile in high-risk neuroblastoma that discriminates between the main groups within high-risk: *MYCN*-amplified and 11q-deleted. Moreover, we demonstrated that some methylated genes, including *CCR7* and *CSF1R*, have prognostic value in 11q-deleted subgroup (8).

Liquid biopsy has emerged as a potentially outstanding tool for spatiotemporal studies of cancer dynamics as well as an accurate monitor of disease (9, 10). In neuroblastoma patients, blood-derived plasma cell-free DNA (cfDNA) has shown its feasibility and accurate representation of the tumor regarding copy number variations (CNVs) (11) and exon mutations (12). cfDNA is typically found as

double-stranded fragments of approximately 150 - 200 base pairs in length, corresponding to the unit size of nucleosome (13). cfDNA is released into the bloodstream by cellular processes involving apoptosis, necrosis and secretion (14). In healthy populations, it is found at a very low concentration, often less than 10 ng per ml of plasma (15), but under some circumstances this amount could increase, including trauma, myocardial infarction, stroke, chronic diseases and cancer. When this cfDNA is released by tumor cells, it is termed circulating tumor DNA (ctDNA) and its levels are related to stage and tumor burden, increasing up to 50 times that of normal levels. Consistent with this notion, a favorable response to cancer treatment is associated with a rapid decrease in blood-based cfDNA concentration in patients with high-risk neuroblastoma (16).

Thus, ctDNA fraction has become a surrogate marker for the staging, prognosis, monitoring response and minimal residual disease, and identification of acquired drug-resistance mechanisms (17). Notably, the distribution patterns of different DNA size occur independently of disease status (16), suggesting that cellular processes involved in DNA fragmentation are unique to the tumor biology in each patient and not to pathological conditions of the disease. The proportion ctDNA/cfDNA is highly variable, ranging from <0.05% (18) to 90% (19), so adequately discriminating between one and the other and determining the suitable threshold is essential to be successful in its analysis. Elevated ctDNA fraction has been reported to be relevant for adequate tumor profiling and for the identification of genetic alterations across cancer types (20). Elevated ctDNA fraction was also found reliable for identifying targetable kinase fusions across cancer types (21). In an ovarian cancer study, whole genomic sequencing-based CNVs were detected in the tumor with a median of 50% of genome altered fraction, but in the ctDNA with a median fraction of 12.7% (22). This plasma genome altered fraction was associated with progression-free survival (PFS), supporting the clinical value of ctDNA fraction. One interesting study on the correlation of metastatic location and ctDNA fraction in colon cancer revealed that, patients with lung-only and peritoneum-only metastatic disease, had significantly lower levels of ctDNA, suggesting decreased ctDNA released and clinical sensitivity depending on sites of metastasis (23). In non-

small cell lung cancer patients, higher ctDNA fraction and detection after initial treatment was associated with shorter PFS, hence identifying patients who may benefit from further therapeutic intervention (24). Importantly, a retrospective analysis across tumor types revealed that ctDNA quantity varied significantly based on patient age, sex, stage, and tumor type, explaining why certain liquid biopsy specimens are more likely to fail sequencing or provide clinically meaningful results (25). Genomic ctDNA profiling has also demonstrated its value in neuroblastoma, showing clonal evolution dynamics in somatic alterations that increase at relapse and therefore, pointing out its use for targeted therapies (12). Recently, ctDNA was reported to be prevalent in children with high-risk neuroblastoma and valuable for follow-up during neuroblastoma treatment (26).

DNA methylation profiling has become a promising approach for sensitive and specific detection of many cancers. Bisulfite conversion of unmethylated CpGs has been the standard method for methylation profiling. Reduced Representation Bisulfite Sequencing (RRBS) is a good method for DNA methylation studies, covering about 3 million CpG sites, with an affordable cost (27). However, current techniques for capturing CpG-rich regions may result in loss of some functionally relevant information. Also, RRBS covers approximately 20% of the total CpG islands in the genome (28) and only 60% of the promoter regions (29). Additionally, this method excludes genes lacking or with a distant CCGG motif. Therefore, use of RRBS could result in failure to obtain complete and relevant information due to the lower coverage of this technique. Another effective approach for targeted methylome studies is the heat enrichment of CpG-rich regions for bisulfite sequencing (Heatrigh-BS) (30). Heatrich-BS allows methylation profiling in highly informative regions, but it fails to capture information on single CpG or small CpG islands. In addition, bisulfite causes DNA degradation, resulting in the loss of information limited in samples with very small amounts of ctDNA. Therefore, several bisulfite conversion-free methods have been developed and optimized for the detection of cfDNA methylation (27). Several bisulfite genomic sequencing studies across neuroblastoma risk groups reported differential methylation profiles of genes that are associated to prognosis (*SCNN1A*, *PRKCDBP*, *KRT19*, *HIST1H3C*, *GNAS*, and a 58 gene signature) (31–33).

Recent studies with immunoprecipitation of cell-free methylated DNA coupled with next-generation sequencing (cfMeDIP-seq) have shown this an effective approach for the analysis of cfDNA methylome from minute quantities of cfDNA (34, 35). However, this technical approach may not detect valuable information in hypomethylated regions relevant to cancer progression. cfDNA fragmentation patterns contain important molecular information linked to tissues of origin and gene expression inference. Recent studies on fragmentomics-based methylation analysis (FRAGMA) have shown the feasibility of using cfDNA cleavage patterns to deduce CpG methylation at single CpG resolution using a deep learning algorithm (36). Moreover, a recent study demonstrates that libraries made using the Enzymatic Methyl-seq (EM-seq), another bisulfite-free method, outperformed bisulfite-converted libraries in all specific measures examined (coverage, duplication, sensitivity, etc.) (37).

In the present article, we use ctDNA from high-risk neuroblastoma patients to compare two conversion methods of unmethylated cytosine, bisulfite and enzymatic conversion, for whole methylome sequencing studies. We also analyze the tumor fraction (ctDNA/cfDNA) content at diagnosis and relapse to establish the suitable threshold for optimal analysis of tumor methylome profile. Several key points for the successful methylome study of high-risk neuroblastoma are indicated in our results.

Material and methods

Patients and samples

A retrospective study was performed in a primary cohort of 86 patients diagnosed with primary high-risk neuroblastoma who underwent treatment between 2007 and 2019. 79 patients were classified in M stage and 7 in L2 stage, with mean age of 42 months at diagnosis. 43 relapsed (the mean time to relapse was 17.5 months), of whom 41 samples were collected. These cases were collected from the archives of Hospital La Fe in Valencia. Clinical characteristics for each patient are summarized in Table 1. Around 1 ml of blood was obtained from neuroblastoma patients. Written informed consent was signed by the patients; when not possible (dead or unreachable patients), the study material was used after decoding in accordance with Spanish law and with the approval of the Institutional Review Board. All procedures were done in accordance with the Helsinki declaration.

Isolation quantification and analysis of ctDNA

Whole blood samples were collected in PAXgene tubes and kept at room temperature for no more than 24 hours before plasma was collected by centrifugation two consecutive times for 15 minutes at 2000xg. Plasma was stored at -80°C until the moment of use. DNA was isolated from 1 ml of blood-derived plasma with QIAamp Circulating Nucleic Acid Kit (QIAGEN). Quantity and quality of isolated ctDNA was determined by using D1000 ScreenTape assay in Agilent 4200 TapeStation. We have also used this method to quantify DNA, focusing on mono-nucleosomal fragments around 100–200 base pairs, but other larger nucleosome sizes were also considered. The median of ctDNA from diagnosis and relapse samples, collected from 1 ml of blood, was 24.2 ng. Quantity of double-stranded DNA was also determined with Qubit (ThermoFisher).

Bisulfite conversion-based method

This method is based on the conversion of unmethylated cytosine to uracil, while methylated cytosines remained unchanged. The QIAseq Methyl Library Kit (QIAseq) was used to prepare libraries from bisulfite-treated DNA samples for whole genome methylation studies using Illumina platforms. QIAseq

TABLE 1 Clinical characteristics of the high-risk neuroblastoma patients included in the study.

Characteristics	INRG		
	M	L2	Total
Number of patients			
	79	7	86
Age at diagnostic in months			
Median	42.03	23.8	41.6
Range	(2.67 - 185.8)	(9.5 - 74.1)	(2.67 - 185.8)
Sex			
Female	32	4	36
Male	47	3	50
Relapse			
Yes (%)	40 (50.1%)	3 (43%)	43 (50%)
No (%)	39 (49.4)	4 (57%)	43 (50%)
Median time to relapse (month)	17.5	20.90	17.5

Methyl Library kit allows DNA inputs as low as 100 pg to deliver high-quality, high-yield libraries for use with Illumina platforms. Libraries were constructed with 10 ng or 20 ng of DNA, as indicated, following the manufacturer recommendations.

Enzymatic methyl-sequencing

NEBNext Enzymatic Methyl-seq (EM-seq) was used for the identification of 5-methylcytosine and 5-hydroxymethylcytosine. 10 or 20 ng starting material of cfDNA, as indicated, were used on a two-step conversion of the cytosines. In the first step TET2 oxidation of 5-methylcytosine and oxidation enhancer of 5-hydroxymethylcytosine provided protection to the modified cytosines from conversion by APOBEC deamination, performed in the second reaction. Ultimately, cytosines are sequenced as thymines and 5-methylcytosines or 5-hydroxymethylcytosines are sequenced as cytosines. The final 8 cycles of PCR library amplification were carried out using the NEB Unique dual index primer pairs (NEBNext multiplex oligos for Illumina).

Sequencing and data analysis of ctDNA methylation and CNV assays

The libraries were sequenced on NovaSeq 6000 (Illumina) in paired-end with a read length of 2x151 bp according to the manufacturer's protocol for dual indexing. Image analysis, base calling and quality scoring of the run are processed using the manufacturer's software Real Time Analysis (RTA 3.3.3) and followed by generation of FASTQ sequence files.

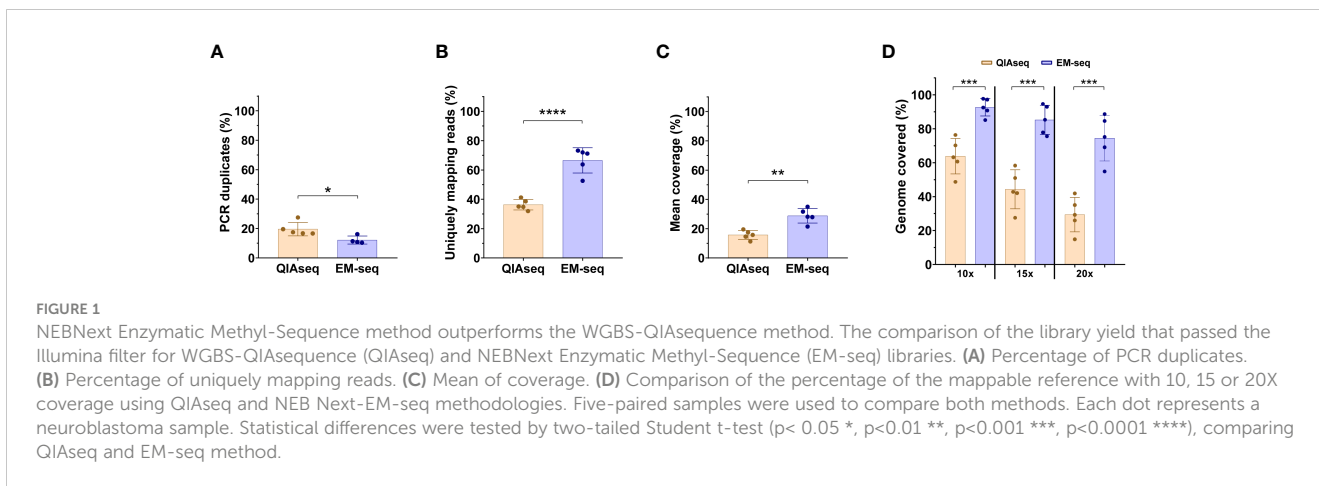
The EM-seq reads were processed using the gemBS pipeline v4.03 using as reference GRCh38. Reads with MAPQ scores < 20 and read pairs mapping to the same start and end points on the

genome were filtered out after the alignment step. The first 5 bases from each read were trimmed before the variant and methylation calling step to avoid artifacts due to end repair. For each sample, CpG sites were selected where both bases were called with a Phred score of at least 20, corresponding to an estimated genotype error level of $\leq 1\%$, and where the total number of reads informative for methylation from both strands combined was ≥ 6 . Sites with $>500\times$ coverage depth were excluded to avoid centromeric/telomeric repetitive regions. Sequencing depth for the analysis of CNV was calculated using samtools v1.15. Liquidhope cohort data is available at Geo database (GSE221317; <https://www.ncbi.nlm.nih.gov/geo/query/acc.cgi?acc=GSE221317>).

Results

EM-seq was more efficient than bisulfite conversion for whole genome methylome sequencing

To gain novel information regarding methylome studies and DNA methylation biomarkers relevant for high-risk neuroblastoma, we assessed the performance of EM-seq vs. bisulfite conversion methods for implementing methylome profiling in liquid biopsies (Figure 1; Supplementary Figure S1). Results from both methodologies indicated an optimal library size and integrity of the ctDNA obtained. However, we obtained higher library concentration (ng/ μ L) with the EM-seq approach (Table 2). Of note, we also compared the use of 10 ng versus 20 ng of DNA, with similar results in terms of the library concentration ($p = 0.57$ for QIAseq; $p = 0.55$ for EM-seq), but again, so we used 10 ng of DNA. The comparison between the QIAseq and the EM-seq approach, performed five to six times higher in the DNA library content for the EM-seq method (Table 2).



Regarding the conversion efficiency, the QIAseq method does not include an internal quality control of conversion; the EM-seq does have this control. Therefore, we compared the conversion rate of unmethylated cytosines by focusing on non-CpG sites (assuming that most of these will be unmethylated). With the EM-seq method, we obtained 99.8% conversion efficiency using this metric, and with QIAseq method we obtained a conversion efficiency of 99%. The comparison of the library yield (Gb generated in the sequencing run) between QIAseq and EM-seq showed similar results (Supplementary Figures S1A, B). Both techniques generated similar amounts of sequencing data with no significant differences, referred to by either total millions of reads (Supplementary Figure S1A), or by Gigabases (Supplementary Figure S1B). Although the amount of sequencing data obtained was similar between the two methods, the EM-seq method showed significant differences in the rest of the parameters evaluated. The EM-seq method yielded a lower proportion of PCR duplicates, thus, reducing the possibility of false positive variant calls (Figure 1A). EM-seq also had a higher percentage of unique mapping reads (Figure 1B), offering a higher mean coverage (Figure 1C) and a higher genome coverage (Figure 1D). The percentages of the mappable references with at least 10x, 15x, or 20x coverage depth are highly uniform for the EM-seq and superior to those obtained with the QIAseq approach (Figure 1D). Thus, our results suggest that the EM-seq is more optimal than the QIAseq method for whole methylome studies.

Electropherogram-based identification of samples with suitable ctDNA content

To determine the best technique for the study of ctDNA methylome from liquid biopsies, DNA was isolated from 1 ml of blood-derived plasma of 126 samples from 86 patients diagnosed with high-risk neuroblastoma, 40 paired samples at diagnosis and at relapse, 44 samples only at diagnosis and 2 samples only at relapse, (Supplementary Table S1). All samples were evaluated with D1000 ScreenTape to determine the quality and quantity of DNA (Supplementary Table S1). Although the electropherogram profile of cfDNA in pediatric tumors, including neuroblastoma, has its use and variability among different biofluids (16), its interpretation as potential reservoir of valuable tumor DNA remains elusive.

To further discriminate when a sample is sufficiently enriched with ctDNA, we combined electropherogram profiles with sequencing-based CNVs. Following the initial diagnosis, we also validated the presence of MYCN amplification or/and 11q deletion in each patient by analyzing sequence-based CNVs from ctDNA (Supplementary Table S1). In addition, we further evaluated the methylation profile of chromosomes, considering a ctDNA-containing sample when hypomethylation values dropped down to 0.25 or lower, resulting in sharp changes in the methylation profiles. Samples with no or highly diluted ctDNA barely showed sharp changes in their methylation profile, displaying a waviness

TABLE 2 Library and size comparison between QIAseq and EM-seq conversion methods.

Gender	Stage	Input ctDNA (ng)	QIAseq		EM-seq	
			Library [ng/ul]	Size (bp)	Library [ng/ul]	Size (bp)
Male	M	20	6.26	326	11.26	304
Male	M	20	6.53	319	102.49	297
Female	M	10	7.7	327	35.79	301
Female	M	20	7.74	324	42.46	302
Male	L2	10	6.84	309	21.27	299

Five-paired samples were used to compare both methods in parallel.

profile ranging between 0.75 and 1 (Supplementary Table S1). *In vitro* enrichment of ctDNA was originally focused on mechanical isolation of mono-nucleosomal fragments (later on defined ctDNA with a median fragment length of 134–144 bp) to improve the ratio between ctDNA and cfDNA (38). In here we used a simplified

approximative method calculating mono-nucleosomal/total cfDNA content as an estimate of ctDNA ratio (Supplementary Table 1).

Samples containing a mono-nucleosomal peak at around 100–200 base pairs, with or without a smaller peak at di-nucleosomal size and sometimes also at tri-nucleosomal size (Figures 2A, B),

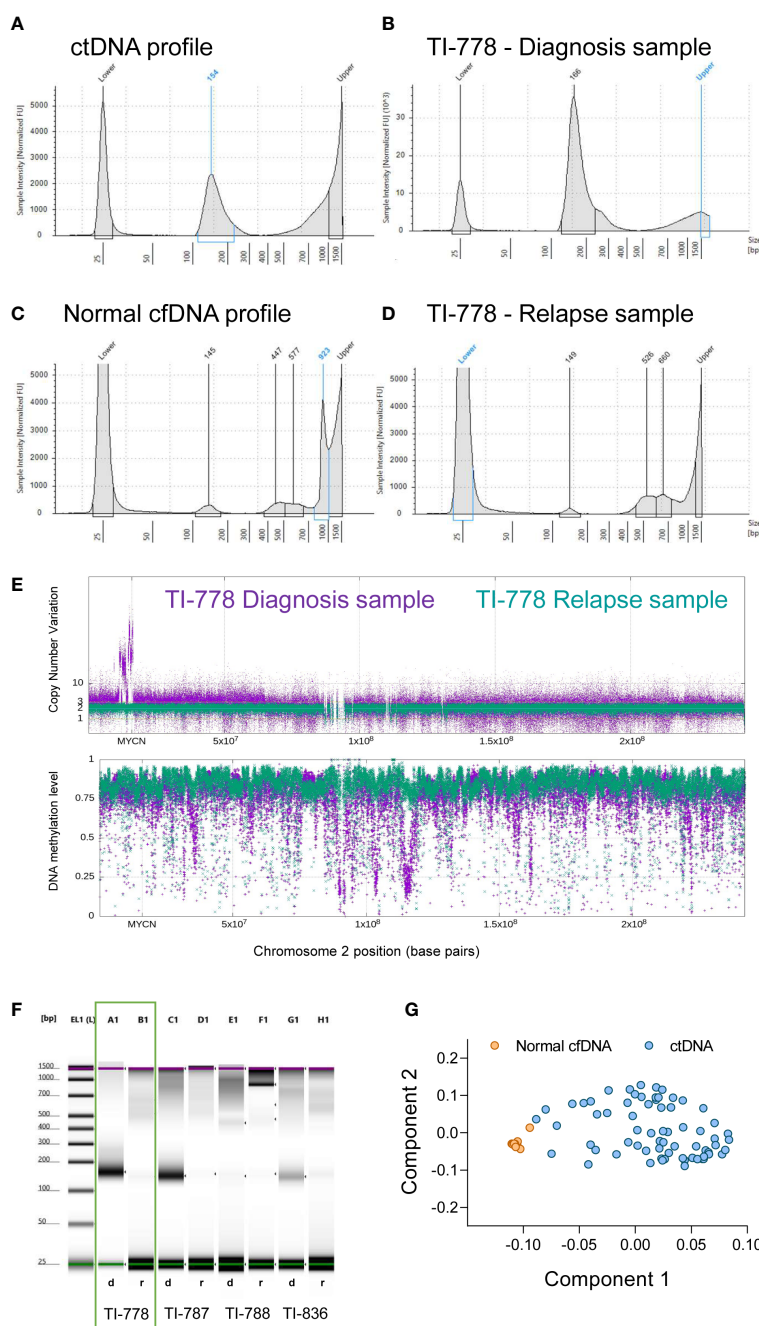


FIGURE 2
 Electropherogram profiles retain relevant information to interpret ctDNA/cfDNA content in blood-derived plasma samples. (A–D) The characteristic profiles in TapeStation electropherograms (mono-nucleosomal peak and higher fragments) allow the discrimination between samples enriched in ctDNA (A, B) and normal cfDNA (C, D). Electropherograms include two picks for the low and high molecular weights (25 and 1500 bp), as indicated, corresponding to the ladder controls used to estimate sizes. Electropherogram images of the paired samples in orange square (patient TI-778) are represented at diagnosis (B) and at relapse (D). (E) Whole genome methylation analyses corroborated that sample TI-778 at diagnosis (in purple) contained valuable tumor DNA, while at relapse (in green) contained mostly normal DNA. (F) Representative electrophoretic runs in a D1000 ScreenTape assay of four paired samples at diagnosis (d) and relapse (r). (G) Principal components model that discriminates tumor DNA-enriched samples that cluster together (blue circles), from normal DNA-containing samples (orange circles).

contained CNVs as detected by sequencing analysis. In addition, the profile of methylation averaged over 1kb bins for these samples and displayed extended regions of hypo-methylation with blocks of methylation extending over many kb with average methylation below 0.5 (Figure 2E, purple trace; Supplementary Figure 2C). In contrast, samples with low content of mono-nucleosomal peak and with high molecular weight DNA contamination, showed an absence of CNVs, with the average methylation profile remaining predominantly above 0.7, with no evidence of extended regions of hypo-methylation below 0.5 (Figure 2E, green trace; Supplementary Figure 2D). These samples without detectable ctDNA or with highly diluted ctDNA based on the absence of mono-nucleosomal peak, the absence of CNVs and by the absence of extended hypomethylation regions below 0.5 were referred to as normal cfDNA (Figure 2C, D). In addition to a rather small mono-nucleosomal peak, normal cfDNA may contain multi-nucleosome peaks with increasing DNA quantities (Figure 2C). Samples of disease-free neuroblastoma patients (at the end of treatment or during subsequent follow-up) lacked the mono-nucleosomal fragment (Supplementary Figures S2A, B), further supporting that the mono-nucleosomal fragment is an indicator of ctDNA content.

The sample for patient TI-778 at the time of diagnosis (purple, upper panel, Figure 2E), exhibited many copies at *MYCN* locus on chromosome 2, confirming the diagnosis with *MYCN* amplification, and depth variations in methylation profile (bottom panel, Figure 2E). However, the relapse profile from the same patient (depicted in green) did not exhibit *MYCN* amplification, nor variation of its methylation profile, suggesting that ctDNA content was low and highly diluted by normal cfDNA, further confirming our previous observations in the TapeStation profiles (Figures 2B, D, F). We evaluated the ctDNA content in samples based on principal component analysis (PCA) of the sequenced methylome in each sample (Supplementary Table S1). Analysis of the Component 1 and Component 2 showed that samples considered to contain normal DNA clustered together, whereas those samples containing significant amounts of ctDNA grouped distinctly from the normal samples (Figure 2G).

Electropherogram profiles were classified as tumor or normal based on their methylome and genomics profiles. Since the mono-nucleosomal peak is considered to be principally of tumor origin (38), we used the electropherogram profile in each sample to calculate the ratio mono-nucleosomal (100-200 pb)/total low molecular weight DNA (100-1000 pb) (Supplementary Table S1). We established a biased cut-off ratio of 10% and noted that it was successful in 95.1% of the cases studied; the prediction failed in only

4 out of 81 samples for which we had CNV and methylation profiles (Supplementary Table S1). For these 4 cases, we also evaluated Qubit quantification (Table 3). We observed that the Qubit quantification in these cases was much greater than the quantified peaks in the electropherogram. One possibility is that the limited range of sizes analyzed by D100 TapeStation do not cover the higher molecular weights of DNA released by cells that succumb by necrosis instead of apoptosis. These results suggest that the contribution to cfDNA by different cellular processes varies in each patient depending on their specific tumor conditions such as size, proliferation, dissemination and others. These results support that analysis of TapeStation electropherograms, combined with total DNA measurements by Qubit, may constitute a relevant tool for determining the presence of ctDNA in a sample.

The comparisons of CNV and hypomethylation profiles, with TapeStation electropherogram profiles was also extended to evaluate the relative quantity of mono-nucleosomal peak as an estimate of the ctDNA content in the sample (Supplementary Figures S2A-D; Supplementary Table S1). The mono-nucleosomal peak was most abundant in most, but not all, ctDNA containing samples, but showed a low concentration when normal cfDNA was prevalent and was diluted with multi-nucleosomal peaks that increased in quantity with their size (Supplementary Figure S2; Supplementary Table S1).

Relapse blood samples contains less ctDNA

The quantification of the total cfDNA (100 – 1000 bp, TapeStation electropherogram) did not exhibit a significant statistical difference between diagnosis and relapse samples (Figure 3A). However, the quantification of mono-nucleosomal fragment size (100-200 bp) showed that samples at diagnosis contained a higher amount of ctDNA (Figure 3B). This increase was further magnified when considering paired diagnosis and relapse samples (Figure 3C). A representative image of TapeStation quantification is shown in Figure 2F, with 4 samples at diagnosis (A1, C1, E1 and G1 wells, Figure 2F) and their corresponding relapse samples (B1, D1, F1 and H1, Figure 2F), and whose mono-nucleosomal quantifications is indicated in Supplementary Table S1. The amount of ctDNA found was higher for samples at diagnosis than for samples at relapse (Figure 3C).

DNA quantification was compared at diagnosis and at relapse (see representative patient TI-778 in wells A1 and B1 in Figure 2F,

TABLE 3 Qubit quantification in ctDNA-containing samples with reduced mono-nucleosomal peak.

Patient	Sampling time	Mono-nucleosomal/Total amount	Prediction based on ratio	PCA clustering	Qubit quantification (ng)
TI-745	Relapse	0.131	Tumor	Normal	815
TI-913	Relapse	0.059	Normal	Tumor	940
TI-1017	Diagnosis	0.066	Normal	Tumor	290
TI-1041	Diagnosis	0.044	Normal	Tumor	287.5

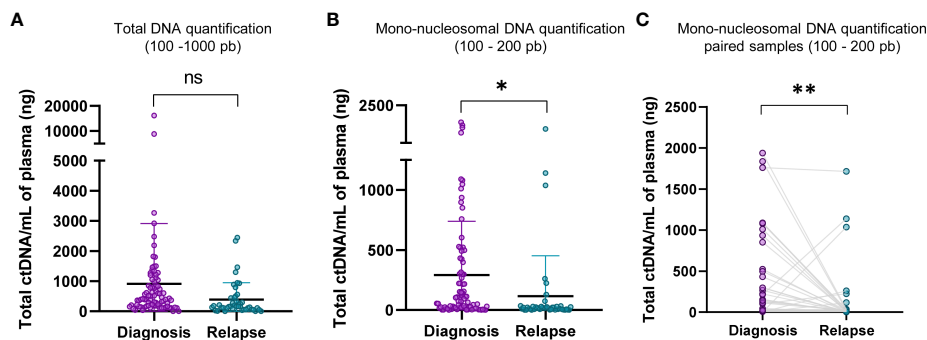


FIGURE 3

Mono-nucleosomal DNA is less abundant in relapse samples. (A) Comparison of total DNA quantifications of fragments within the range of D1000 ScreenTape assays (100 – 1000 bp) between diagnosis and relapse samples. (B) Comparison of mono-nucleosomal DNA quantifications (100 – 200 bp) between diagnosis and relapse samples. The quantification corresponding to nucleosomal fragment, 100 – 200 bp, to diagnosis and relapse in paired samples was shown in (C). Statistical differences were tested by two-tailed Student t-test (ns, not significant $p > 0.05$, $p < 0.05$ *, $p < 0.01$ **).

orange square; quantification for all patients is shown in [Supplementary Table S1](#)). Electropherogram profile at diagnosis (Figure 2B) coincided with the expected profile for a sample containing valuable ctDNA (Figure 2A), with a major peak at mono-nucleosomal size and in some samples with bi- and tri-nucleosomal peaks that were reduced in quantity as the size of fragments increased. At relapse, samples more frequently showed a small mono-nucleosomal peak diluted by other multi-nucleosomal peaks (see representative patient TI-778 in Figure 2E). In parallel, sequencing data was used to estimate CNV and confirmed the original status for *MYCN* amplification, 11q deletion ([Supplementary Table S1](#)), or other segmental chromosomal aberrations (SCA). Those cases that did not have any SCA were considered as highly diluted with normal cfDNA, and their normal assessment was further confirmed by the reduced hypomethylation profiles derived from the sequencing (Figure 2E; [Supplementary Table S1](#)) and by the tumor-independent clustering in the PCA (Figure 2G; [Supplementary Table S1](#)). These distinct electropherogram profiles demonstrate that samples at relapse have a lower ctDNA content per ml of blood than samples taken at the time of diagnosis.

Discussion

Analysis of ctDNA methylation has emerged as a promising tool with many potential clinical applications in the field of neuroblastoma (16). However, in attempting to apply this approach to pediatric patients, we previously encountered limitations with the ctDNA quantity and/or quality (ctDNA was present but significantly diluted with normal cfDNA) to perform methylation studies. These limitations arising from normal/tumor origin of cfDNA are relevant for making decisions regarding whether to submit a sample to subsequent techniques and analyses. Given the relevance of resolving these technical obstacles, we assessed two cytosine-conversion techniques for ctDNA methylome studies, and found that the EM-seq method performed better than the bisulfite technique.

Both RRBS and whole genome methyl-sequencing, allow the identification of pan-methylation status of cytosines with very low input amount of DNA, in contrast to array-based analysis that requires over 100 ng of DNA, an unattainable amount for liquid biopsy samples in most of pediatric cases. In our search to identify a suitable technique for whole genome methyl-sequencing study from limited amounts of ctDNA (10 ng), we evaluated two methods, the QIaseq, based on the standard genome bisulfite conversion, and EM-seq methods, based on two-step enzymatic conversion process. Our comparison between the different techniques indicates that, although conversion efficiency, library size and integrity obtained were optimal in both methodologies, we achieved higher library concentration, five to six times higher, with the EM-seq approach (Table 2). EM-seq also demonstrated better efficiency when we evaluated the proportion of PCR duplicates, the percentage of uniquely mapping reads, the mean coverage and genome covered (Figures 1A-D), supporting the use of EM-seq over QIaseq method for ctDNA-based methylome studies. In agreement with our results, comparisons between EM-seq and bisulfite methods using genomic DNA methylome analysis showed that EM-seq performed better for library and sequencing quality; the EM-seq method produced larger insert sizes, higher alignment rates and higher library complexity with lower duplication rate as well as higher CpG coverage (39).

Although currently there are no standardization procedures for the routine clinical application of ctDNA/cfDNA analysis, several studies have highlighted the significance of variability and integrity of samples to ensure high-quality molecular tests (40–43). The pipeline gemBS used for processing EM-seq reads, enables the analysis of methylated DNA and CNVs, as well as single nucleotide variants, but not rearrangements. Nonetheless, single nucleotide variants were not the focus in this study. Our results reveal that evaluation of TapeStation electropherogram profiles offers a reliable approach to discriminate ctDNA from normal cfDNA. In our studies, 0.1 was established as the minimal ratio of ctDNA to normal cfDNA, ensuring that the tumor sample is sufficiently represented to perform subsequent methylome analysis. This is a crucial step for selecting samples that contain adequate ctDNA/normal cfDNA. A recent report suggests that total cfDNA concentrations in blood plasma from

patients with high-risk neuroblastoma were higher than in healthy controls (44). However, in our cohort, 13 samples with apparently high concentration of cfDNA were classified as normal cfDNA or highly diluted ctDNA (i.e. patient TI-0572 with *MYCN* amplification at diagnosis had only 3 copies at relapse, with no other genetic or epigenetic alterations) after sequencing analysis. In healthy individuals, cfDNA is very low, averaging 10 to 15 ng per milliliter (45). In oncological patients, ctDNA can fluctuate from <0.1% to >90% of the cfDNA (46). We noted that cfDNA samples containing useful ctDNA (as determined by CNVs, hypomethylation profiles and PCA clustering) are enriched in mono-nucleosomal fragments (100–200 bp). In contrast, the presence of increasing amounts of multi-nucleosomal peaks (around 600 and 1000 bp) corresponding to four to six nucleosomes suggest dilution by normal cfDNA, except when high molecular weight DNA is present that may be secreted by tumor cells *via* alternative cellular processes. These distinct nucleosomal profiles facilitate identification of samples with high tumoral content which are appropriate for subsequent genomics procedures.

The origin of ctDNA is thought to be dependent on three cellular processes: apoptosis, necrosis and active cellular secretion (17). These different mechanisms by which ctDNA is liberated may contribute to the patient-specific differences and the fluctuating profiles that we observed in the electropherograms. In contrast to the low range of the apoptotic DNA ladder, necrosis is thought to generate ctDNA fragments generally larger than 10,000 bp, which is out of the range of detection by the TapeStation chips but can be quantified by other quality control techniques such as Qubit (Table 3). Interestingly, cfDNA fragments in the range of 1,000–3,000 bp are associated with active cellular secretion processes (47), and thus, these fragments may also be secreted by healthy cells (i.e. white cells in the blood) as a result of specific conditions of the patient. Tumor-specific alterations have been identified and monitored during disease progression in liquid biopsies from pediatric patients with high-risk neuroblastoma (44), as well as in adult tumors such as endometrial cancer (48), follicular lymphoma (49), non-small cell lung cancer (50), breast cancer (51), among others (reviewed in (52)). Our results in high-risk neuroblastoma patients provide support for the early evaluation of valuable ctDNA content in liquid biopsy samples and represent an approach that could be extrapolated to other oncological patients.

CNV analysis derived from whole-genome methyl sequencing indicated that ctDNA was diluted with normal cfDNA in 13 samples (i.e., patient TI-0572, as previously discussed). In addition, the hypomethylation profile also enabled us to discriminate between tumor and normal cfDNA containing samples. DNA methylation changes are similar in most cells of a tumor but in contrast, the manifestations of gene mutations are more heterogeneous within the same tumor (53). Thus, the abnormal distribution of DNA methylation in our neuroblastoma patients, characterized mainly by a sharp methylation dropdown in discrete chromosomal regions, was also a useful tool to identify tumor profiles. The combination of ctDNA hypomethylation with CNVs analysis for further enhancement of the detection of at least one type of aberration to define an abnormality, was previously shown to have a sensitivity of 87% with a specificity of 88% in hepatocellular carcinoma (54). Thus, our results extend the application of ctDNA analysis to the detection and monitoring of high-risk neuroblastoma.

One interesting observation from our studies is that relapsed samples usually contained lower amounts of ctDNA (referred as to mono-nucleosomal peak) per ml of blood than their paired samples at diagnosis. Consistent with this, ctDNA at relapse was more easily masked by normal cfDNA, even though all samples were carefully subjected to the same technical procedures. Although we do not yet have a clear explanation for these findings, one possibility is that high-risk neuroblastoma at relapse is a more disseminated disease associated with less hypoxia. Therefore, hypoxia-associated processes such as apoptosis and necrosis, are also reduced and thus, less ctDNA is released into the bloodstream than at diagnosis. Alternatively, neuroblastoma relapses are more frequently found in bone marrow, which could represent a barrier for liberating tumor DNA to the bloodstream.

Collectively, our results support the use of cytosine enzymatic conversion over chemical modification as an optimal method to study ctDNA methylome with as little as 10 ng of DNA and provide a conceptual tool for the electropherogram-based detection of samples with useful ctDNA content for subsequent studies.

Data availability statement

The datasets presented in this study can be found in online repositories. The names of the repository/repositories and accession number(s) can be found in the article/Supplementary Material.

Ethics statement

La Fe Research Ethics Committee approved this project, reference number 2018-02-09. Written informed consent to participate in this study was provided by the participants' legal guardian/next of kin.

Author contributions

ET: Conception and design, collection and/or assembly of data, data analysis and interpretation, manuscript writing. AJ-R, GP, MG: Collection and/or assembly of data, data analysis and interpretation. VC, AC: Conception and design data analysis and interpretation, manuscript writing. SH: Conception and design data analysis and interpretation, manuscript writing. JF: Financial support, conception and design, collection and/or assembly of data, data analysis and interpretation, manuscript writing, coordination. All authors contributed to the article and approved the submitted version.

Funding

Supported by TRANSCAN-2 consortium LIQUIDHOPE by Fundación Científica de la Asociación Española Contra el Cáncer (TRNSC18001FON), by Spanish Ministry of Science and

Innovation (PID2020-119323RB-I00 grant) and by “Sumemos muchas manos por los niños enfermos” non-profit organization.

Acknowledgments

We are grateful to D. Ramal (Pediatric Oncology Clinical Trials Unit, University Hospital La Fe) for update and support on patients' data analyzed in Table 1.

Conflict of interest

The authors declare that the research was conducted in the absence of any commercial or financial relationships that could be construed as a potential conflict of interest.

References

- Matthay KK, Maris JM, Schleiermacher G, Nakagawara A, Mackall CL, Diller L, et al. Neuroblastoma. *Nat Rev Dis Prim* (2016) 2:16078. doi: 10.1038/nrdp.2016.78
- Van Arendonk KJ, Chung DH. Neuroblastoma: tumor biology and its implications for staging and treatment. *Child* (2019) 6(1):12. doi: 10.3390/children6010012
- Maris JM. Recent advances in neuroblastoma. *N Engl J Med* (2010) 362(23):2202–11. doi: 10.1056/NEJMra0804577
- Gröbner SN, Worst BC, Weischenfeldt J, Buchhalter I, Kleinheinz K, Rudneva VA, et al. The landscape of genomic alterations across childhood cancers. *Nat* (2018) 555(7696):321–7. doi: 10.1038/nature25480
- Pugh TJ, Morozova O, Attiyeh EF, Asgharzadeh S, Wei JS, Auclair D, et al. The genetic landscape of high-risk neuroblastoma. *Nat Genet* (2013) 45(3):279–84. doi: 10.1038/ng.2529
- Sanmartín E, Yáñez Y, Fornés-Ferrer V, Zugaza JL, Cañete A, Castel V, et al. TIAM1 variants improve clinical outcome in neuroblastoma. *Oncotarget*. (2017) 8(28):45286–97. doi: 10.18632/oncotarget.16787
- Fetahu IS, Taschner-Mandl S. Neuroblastoma and the epigenome. *Cancer Metastasis Rev* (2021) 40(1):173–89. doi: 10.1007/s10555-020-09946-y
- Trinidad EM, Vidal E, Coronado E, Esteve-Codina A, Castel V, Cañete A, et al. Liquidhope: methylome and genomic profiling from very limited quantities of plasma-derived DNA. *Brief Bioinform* (2023) 24(1):bbac575. doi: 10.1093/bib/bbac575
- Pinzani P, D'Argenio V, Del R, Pellegrini C, Cucchiara F, Salviani F, et al. Updates on liquid biopsy: current trends and future perspectives for clinical application in solid tumors. *Clin Chem Lab Med* (2021) 59(7):1181–200. doi: 10.1515/cclm-2020-1685
- Crowley E, Di Nicolantonio F, Loupakis F, Bardelli A. Liquid biopsy: monitoring cancer-genetics in the blood. *Nat Rev Clin Oncol* (2013) 10(8):472–84. doi: 10.1038/nrclinonc.2013.110
- Chicard M, Boyault S, Daage LC, Richer W, Gentien D, Pierron G, et al. Genomic copy number profiling using circulating free tumor DNA highlights heterogeneity in neuroblastoma. *Clin Cancer Res* (2016) 22(22):5564–73. doi: 10.1158/1078-0432.CCR-16-0500
- Chicard M, Colmet-Daage L, Clement N, Danzon A, Bohec M, Bernard V, et al. Whole-exome sequencing of cell-free DNA reveals temporo-spatial heterogeneity and identifies treatment-resistant clones in neuroblastoma. *Clin Cancer Res* (2018) 24(4):939–49. doi: 10.1158/1078-0432.CCR-17-1586
- Lo YMD, Chan KCA, Sun H, Chen EZ, Jiang P, Lun FMF, et al. Maternal plasma DNA sequencing reveals the genome-wide genetic and mutational profile of the fetus. *Sci Transl Med* (2010) 2(61):61ra91. doi: 10.1126/scitranslmed.3001720
- Thierry AR, El Messaoudi S, Gahan PB, Anker P, Stroun M. Origins, structures, and functions of circulating DNA in oncology. *Cancer Metastasis Rev* (2016) 35(3):347–76. doi: 10.1007/s10555-016-9629-x
- Giacona MB, Ruben GC, Iczkowski KA, Roos TB, Porter DM, Sorenson GD. Cell-free DNA in human blood plasma: length measurements in patients with pancreatic cancer and healthy controls. *Pancreas* (1998) 17(1):89–97. doi: 10.1097/00006676-199807000-00012
- Lodrimi M, Wünschel J, Thole-kliesch TM, Grimaldi M, Sprüssel A, Linke RB, et al. Circulating cell-free DNA assessment in biofluids from children with neuroblastoma

Publisher's note

All claims expressed in this article are solely those of the authors and do not necessarily represent those of their affiliated organizations, or those of the publisher, the editors and the reviewers. Any product that may be evaluated in this article, or claim that may be made by its manufacturer, is not guaranteed or endorsed by the publisher.

Supplementary material

The Supplementary Material for this article can be found online at: <https://www.frontiersin.org/articles/10.3389/fonc.2023.1037342/full#supplementary-material>

demonstrates feasibility and potential for minimally invasive molecular diagnostics. *Cancers (Basel)* (2022) 14(9):2080. doi: 10.3390/cancers14092080

17. Bronkhorst AJ, Ungerer V, Holdenrieder S. The emerging role of cell-free DNA as a molecular marker for cancer management. *Biomol Detect Quantif* (2019) 17:100087. doi: 10.1016/j.bdq.2019.100087

18. Diehl F, Schmidt K, Choti MA, Romans K, Goodman S, Li M, et al. Circulating mutant DNA to assess tumor dynamics. *Nat Med* (2008) 14(9):985–90. doi: 10.1038/nm.1789

19. Jahr S, Hentze H, Englisch S, Hardt D, Fackelmayer FO, Hesch RD KR. DNA Fragments in the blood plasma of cancer patients: quantitations and evidence for their origin from apoptotic and necrotic cells. *Cancer Res* (2021) 61(4):1659–65.

20. Husain H, Pavlick DC, Fendler BJ, Madison RW, Decker B, Gjoerup O, et al. Tumor fraction correlates with detection of actionable variants across > 23,000 circulating tumor DNA samples. *JCO Precis Oncol* (2022) 6:e2200261. doi: 10.1200/PO.22.00261

21. Lee JK, Hazar-Rethinam M, Decker B, Gjoerup O, Madison RW, Lieber DS, et al. The pan-tumor landscape of targetable kinase fusions in circulating tumor DNA. *Clin Cancer Res* (2022) 28(4):728–37. doi: 10.1158/1078-0432.CCR-21-2136

22. Sabatier R, Garnier S, Guille A, Carbuca N, Pakradouni J, Adelaide J, et al. Whole-genome/exome analysis of circulating tumor DNA and comparison to tumor genomics from patients with heavily pre-treated ovarian cancer: subset analysis of the PERMED-01 trial. *Front Oncol* (2022), 12. doi: 10.3389/fonc.2022.946257

23. Bando H, Nakamura Y, Taniguchi H, Shiozawa M, Yasui H, Esaki T, et al. Effects of metastatic sites on circulating tumor DNA in patients with metastatic colorectal cancer. *JCO Precis Oncol* (2022) 6(6):e2100535. doi: 10.1200/PO.21.00535

24. Gale D, Heider K, Ruiz-Valdepenas A, Hackinger S, Perry M, Marsico G, et al. Residual ctDNA after treatment predicts early relapse in patients with early-stage non-small cell lung cancer. *Ann Oncol Off J Eur Soc Med Oncol* (2022) 33(5):500–10. doi: 10.1016/j.annonc.2022.02.007

25. Huang RSP, Xiao J, Pavlick DC, Guo C, Yang L, Jin DX, et al. Circulating cell-free DNA yield and circulating-tumor DNA quantity from liquid biopsies of 12 139 cancer patients. *Clin Chem* (2021) 67(11):1554–66. doi: 10.1093/clinchem/hvab176

26. Bosse KR, Giudice AM, Lane MV, McIntyre B, Schurch PM, Pascual-Pasto G, et al. Serial profiling of circulating tumor DNA identifies dynamic evolution of clinically actionable genomic alterations in high-risk neuroblastoma. *Cancer Discovery* (2022) 12(12):2800–19. doi: 10.1158/2159-8290.CD-22-0287

27. Luo H, Wei W, Ye Z, Zheng J, Xu Rh. Liquid biopsy of methylation biomarkers in cell-free DNA. *Trends Mol Med* (2021) 27(5):482–500. doi: 10.1016/j.molmed.2020.12.011

28. Beck D, Ben Maamar M, Skinner MK. Genome-wide CpG density and DNA methylation analysis method (MeDIP, RRBS, and WGBS) comparisons. *Epigenetics* (2022) 17(5):518. doi: 10.1080/15592294.2021.1924970

29. Sun Z, Cunningham J, Slager S, Kocher JP. Base resolution methylome profiling: considerations in platform selection, data preprocessing and analysis. *Epigenomics* (2015) 7(5):813–28. doi: 10.2217/epi.15.21

30. Cheruba E, Viswanathan R, Wong PM, Womersley HJ, Han S, Tay B, et al. Heat selection enables highly scalable methylome profiling in cell-free DNA for noninvasive monitoring of cancer patients. *Sci Adv* (2022) 8(36):eabn4030. doi: 10.1126/sciadv.abn4030

31. Carén H, Djos A, Nethander M, Sjöberg RM, Kogner P, Enström C, et al. Identification of epigenetically regulated genes that predict patient outcome in neuroblastoma. *BMC Cancer* (2011) 11:66. doi: 10.1186/1471-2407-11-66
32. Kumar RMR, Schor NF. Methylation of DNA and chromatin as a mechanism of oncogenesis and therapeutic target in neuroblastoma. *Oncotarget* (2018) 9(31):22189–98. doi: 10.18632/oncotarget.25084
33. Okae H, Chiba H, Hiura H, Hamada H, Sato A, Utsunomiya T, et al. Genome-wide analysis of DNA methylation dynamics during early human development. *PLoS Genet* (2014) 10(12):e1004868. doi: 10.1371/journal.pgen.1004868
34. Shen SY, Singhanian R, Fehrer G, Chakravarthy A, Roehrl MHA, Chadwick D, et al. Sensitive tumour detection and classification using plasma cell-free DNA methylomes. *Nature* (2018) 563(7732):579–83. doi: 10.1038/s41586-018-0703-0
35. Chen S, Petricca J, Ye W, Guan J, Zeng Y, Cheng N, et al. The cell-free DNA methylome captures distinctions between localized and metastatic prostate tumors. *Nat Commun* (2022) 13(1):6467. doi: 10.1038/s41467-022-34012-2
36. Zhou Q, Kang G, Jiang P, Qiao R, Lam WKJ, Yu SCY, et al. Epigenetic analysis of cell-free DNA by fragmentomic profiling. *Proc Natl Acad Sci U.S.A.* (2022) 119(44):e2209852119. doi: 10.1073/pnas.2209852119
37. Vaisvila R, Ponnaluri VKC, Sun Z, Langhorst BW, Saleh L, Guan S, et al. Enzymatic methyl sequencing detects DNA methylation at single-base resolution from picograms of DNA. *Genome Res* (2021) 31(7):1280–9. doi: 10.1101/gr.266551.120
38. Underhill HR, Kitzman JO, Hellwig S, Welker NC, Daza R, Baker DN, et al. Fragment length of circulating tumor DNA. *PLoS Genet* (2016) 12(7):e1006162. doi: 10.1371/journal.pgen.1006162
39. Han Y, Zheleznyakova GY, Marincevic-Zuniga Y, Kakhki MP, Raine A, Needhamsen M, et al. Comparison of EM-seq and PBAT methylome library methods for low-input DNA. *Epigenetics* (2022) 17(10):1195–204. doi: 10.1080/15592294.2021.1997406
40. Trigg RM, Martinson LJ, Parpart-Li S, Shaw JA. Factors that influence quality and yield of circulating-free DNA: a systematic review of the methodology literature. *Heliyon*. (2018) 4(7):e00699. doi: 10.1016/j.heliyon.2018.e00699
41. Volckmar AL, Sültmann H, Riediger A, Fioretos T, Schirmacher P, Endris V, et al. A field guide for cancer diagnostics using cell-free DNA: from principles to practice and clinical applications. *Genes Chromosomes Cancer* (2018) 57(3):123–39. doi: 10.1002/gcc.22517
42. Lampignano R, Neumann MHD, Weber S, Klotten V, Herdean A, Voss T, et al. Multicenter evaluation of circulating cell-free DNA extraction and downstream analyses for the development of standardized (Pre)analytical work flows. *Clin Chem* (2020) 66(1):149–60. doi: 10.1373/clinchem.2019.306837
43. Cisneros-Villanueva M, Hidalgo-Pérez L, Rios-Romero M, Cedro-Tanda A, Ruiz-Villavicencio CA, Page K, et al. Cell-free DNA analysis in current cancer clinical trials: a review. *Br J Cancer* (2022) 126(3):391–400. doi: 10.1038/s41416-021-01696-0
44. Lodrini M, Graef J, Thole-Kliesch TM, Astrahantseff K, Sprussel A, Grimaldi M, et al. Targeted analysis of cell-free circulating tumor DNA is suitable for early relapse and actionable target detection in patients with neuroblastoma. *Clin Cancer Res* (2022) 28(9):1809–20. doi: 10.1158/1078-0432.CCR-21-3716
45. Leon SA, Shapiro B, Sklaroff DM, Yaros MJ. Free DNA in the serum of cancer patients and the effect of therapy. *Cancer Res* (1977) 37(3):646–50.
46. Corcoran RB, Chabner BA. Application of cell-free DNA analysis to cancer treatment. *N Engl J Med* (2018) 379(18):1754–65. doi: 10.1056/NEJMra1706174
47. Bronkhorst AJ, Wentzel JF, Aucamp J, van Dyk E, du Plessis L, Pretorius PJ. Characterization of the cell-free DNA released by cultured cancer cells. *Biochim Biophys Acta - Mol Cell Res* (2016) 1863(1):157–65. doi: 10.1016/j.bbamcr.2015.10.022
48. Ashley CW, Selenica P, Patel J, Wu M, Nincevic J, Lakhman Y, et al. High-sensitivity mutation analysis of cell-free DNA for disease monitoring in endometrial cancer. *Clin Cancer Res* (2022) 29(2):OF1–12. doi: 10.1158/1078-0432.CCR-22-1134/709202/High-Sensitivity-Mutation-Analysis-of-Cell-Free
49. Fernández-Miranda I, Pedrosa L, Llanos M, Franco FF, Gómez S, Martín-Acosta P, et al. Monitoring of circulating tumor DNA predicts response to treatment and early progression in follicular lymphoma: results of a prospective pilot study. *Clin Cancer Res* (2023) 29(1):209–20. doi: 10.1158/1078-0432.CCR-22-1654
50. Wang S, Li M, Zhang J, Xing P, Wu M, Meng F, et al. Circulating tumor DNA integrating tissue clonality detects minimal residual disease in resectable non-small-cell lung cancer. *J Hematol Oncol* (2022) 15(1):137. doi: 10.1186/s13045-022-01355-8
51. Cailleux F, Agostinetti E, Lambertini M, Rothé F, Wu H-T, Balcioglu M, et al. Circulating tumor DNA after neoadjuvant chemotherapy in breast cancer is associated with disease relapse. *JCO Precis Oncol* (2022) 6(6):e2200148. doi: 10.1200/PO.22.00148
52. Duffy MJ, Crown J. Circulating tumor DNA as a biomarker for monitoring patients with solid cancers: comparison with standard protein biomarkers. *Clin Chem* (2022) 68(11):1381–90. doi: 10.1093/clinchem/hvac121
53. Baylin SB, Jones PA. A decade of exploring the cancer epigenome - biological and translational implications. *Nat Rev Cancer* (2011) 11(10):726–34. doi: 10.1038/nrc3130
54. Allen Chan KC, Jiang P, Chan CWM, Sun K, Wong J, Hui EP, et al. Noninvasive detection of cancer-associated genome-wide hypomethylation and copy number aberrations by plasma DNA bisulfite sequencing. *Proc Natl Acad Sci U.S.A.* (2013) 110(47):18761–8. doi: 10.1073/pnas.1313995110